How to cite: *Angew. Chem. Int. Ed.* **2024**, *63*, e202403494
doi.org/10.1002/anie.202403494

2D Semiconductors

Trifluoromethylation of 2D Transition Metal Dichalcogenides: A Mild Functionalization and Tunable p-Type Doping Method

Brendan Kerwin, Stephanie E. Liu, Tumpa Sadhukhan, Anushka Dasgupta, Leighton O. Jones, Rafael López-Arteaga, Thomas T. Zeng, Antonio Facchetti, George C. Schatz, Mark C. Hersam,* and Tobin J. Marks**

Abstract: Chemical modification is a powerful strategy for tuning the electronic properties of 2D semiconductors. Here we report the electrophilic trifluoromethylation of 2D WSe_2 and MoS_2 under mild conditions using the reagent trifluoromethyl thianthrenium triflate (TTT). Chemical characterization and density functional theory calculations reveal that the trifluoromethyl groups bind covalently to surface chalcogen atoms as well as oxygen substitution sites. Trifluoromethylation induces p-type doping in the underlying 2D material, enabling the modulation of charge transport and optical emission properties in WSe_2. This work introduces a versatile and efficient method for tailoring the optical and electronic properties of 2D transition metal dichalcogenides.

Introduction

Two-dimensional (2D) materials are promising materials for next-generation electronic devices. As a consequence of their ultrathin dimensions and dangling-bond-free interfaces, 2D materials offer the opportunity for continued device scaling while avoiding the short-channel effects that hinder bulk semiconductors.[1,2] In addition, 2D materials are highly sensitive to their environment, making them suitable for "More than Moore" devices that respond to external stimuli.[2–4] Within the expanding family of 2D materials, transition metal dichalcogenides (TMDCs) such as WSe_2 and MoS_2 have emerged as prototypical 2D semiconductors with high mobility and strong current modulation in field-effect transistors (FETs).[5–8] In addition to favorable device performance, these materials have attracted attention in the field of quantum information science for their rich photophysics and bright emission at the monolayer limit.[9,10]

Surface doping is an emerging strategy for tuning the carrier concentration in 2D TMDCs. Molecular species adsorbed on 2D materials induce strong doping through charge transfer and/or dipolar interactions.[2,3,11–17] Reactants that form covalent bonds to the surface, rather than simply physisorbing, are particularly advantageous as they are more stable following exposure to heat, solvents, and ambient moisture and oxygen. Of particular interest are reagents that would react with and modify charge transport in WSe_2, since this material shows both n-type and p-type transport for complementary metal-oxide-semiconductor (CMOS) applications.[5–8,18–21] However, many reports of covalent functionalization of TMDCs, such as pre-activation by conversion to 1T phase[22–24] or the use of radical-based diazonium reagents,[25–27] rely on harsh reaction conditions that may damage and/or significantly alter the crystal lattice. Recently, pioneering work by Pérez and co-workers demonstrated that mild electrophiles such as maleimides react with the surface of MoS_2 and other TMDCs, in analogy to thiol-maleimide "click" chemistry.[28,29] The maleimide functionalization approach introduces significant electron doping in MoS_2 and reduces barriers to charge injection in the contact region.[30] These findings motivate the search for other electrophilic reagents that functionalize and dope TMDCs without the use of harsh reaction conditions.

Here we report the functionalization of 2D WSe_2 and MoS_2 using trifluoromethyl thianthrenium triflate (TTT), an electrophilic trifluoromethylation reagent recently reported by Ritter and co-workers for use in organic synthesis.[31] This

[*] B. Kerwin, Prof. T. Sadhukhan, Dr. L. O. Jones, Prof. A. Facchetti, Prof. G. C. Schatz, Prof. M. C. Hersam, Prof. T. J. Marks
Department of Chemistry and the Materials Research Center, Northwestern University
2145 Sheridan Road, Evanston IL-60208-3113 (USA)
E-mail: t-marks@northwestern.edu
m-hersam@northwestern.edu
g-schatz@northwestern.edu

S. E. Liu, A. Dasgupta, Dr. R. López-Arteaga, T. T. Zeng, Prof. M. C. Hersam, Prof. T. J. Marks
Department of Materials Science and Engineering and the Materials Research Center, Northwestern University
2220 Campus Drive, Evanston IL-60208-3108 (USA)

Prof. T. Sadhukhan
Department of Chemistry, SRM Institute of Science and Technology
Kattankulathur, Tamil Nadu, 603203, India

Prof. A. Facchetti
School of Materials Science and Engineering, Georgia Institute of Technology
Atlanta, Georgia 30332, United States

Prof. M. C. Hersam
Department of Electrical and Computer Engineering, Northwestern University
2145 Sheridan Road, Evanston IL-60208-3113 (USA)

reagent is synthesized in a simple one-step procedure and used under ambient conditions without the need for special precautions or complex synthetic procedures. We show that TTT reacts under mild conditions with exfoliated WSe_2 and MoS_2 to give a self-limited surface layer of covalently bound trifluoromethyl groups, which are characterized by X-ray photoelectron spectroscopy (XPS), solid-state ^{19}F magic-angle spinning nuclear magnetic resonance (MAS NMR) spectroscopy, atomic force microscopy (AFM), time-of-flight secondary ion mass spectrometry (ToF-SIMS), Raman spectroscopy, and density functional theory (DFT) electronic structure calculations. Using proof-of-concept FET studies, we show that trifluoromethylation induces tunable p-type doping of WSe_2 and MoS_2. Moreover, we demonstrate through low-temperature photoluminescence (PL) studies that this doping can be used to tune the contributions of excitonic species to the emission of WSe_2. Overall, this work demonstrates that the mild solution-based chemistry of TTT enables facile and scalable p-type doping of 2D TMDCs.

Results and Discussion

Dispersions of few-layer WSe_2 were prepared using cosolvent liquid-phase exfoliation in 2:1 ethanol/water. Cosolvent exfoliation avoids the use of surfactants to stabilize the WSe_2 dispersion, ensuring that the surfaces of the nanosheets are free of adsorbates that could interfere with surface reactions.[32] Following solvent exchange to acetonitrile, TTT was added to produce a dispersion of few-layer WSe_2 in 10 mM TTT in acetonitrile (Figure 1a). This dispersion was stirred for 4 hours at room temperature, then collected by filtration and washed with excess acetonitrile to remove side products and physisorbed starting material. This technique was scaled up to produce sufficient quantities of functionalized WSe_2-CF_3 powder for analysis with XPS and solid-state ^{19}F MAS NMR.

XPS measurements provide initial evidence for CF_3 group chemisorption on WSe_2. Following functionalization with TTT, a peak appears in the F1s region (Figure 1b). The binding energy of 688 eV is consistent with fluorinated organic compounds, including trifluoromethyl groups.[33] The Se3d peak of pristine WSe_2 shows an overlapping doublet with the $3d_{5/2}$ component centered at 55 eV. This doublet remains in the functionalized material, but deconvolution of the broadened Se3d signal reveals the presence of a new Se species at a higher binding energy. The higher binding energy of the new doublet is consistent with the binding of CF_3 groups to surface Se sites, which is expected to involve electron donation from the Se to the electrophilic CF_3 in analogy to the reaction between TTT and thiols.[31] To determine the density of surface-bound CF_3 groups, we applied the trifluoromethylation reaction to large-area monolayer WSe_2 sample. Quantification of the XPS F1s and Se3d peaks shows that surface coverage increases with reaction time, with a 4-hour reaction giving a density of roughly 1 CF_3 group for every 13 surface Se sites (Figure S1).

Next, we used solid-state ^{19}F MAS NMR spectroscopy to characterize the atomic-scale structure of the functionalized material. ^{19}F is a highly sensitive NMR-active $I = {}^1/_2$ nucleus with nearly 100 % isotopic abundance, which allows the detection of fluorinated species even at relatively low

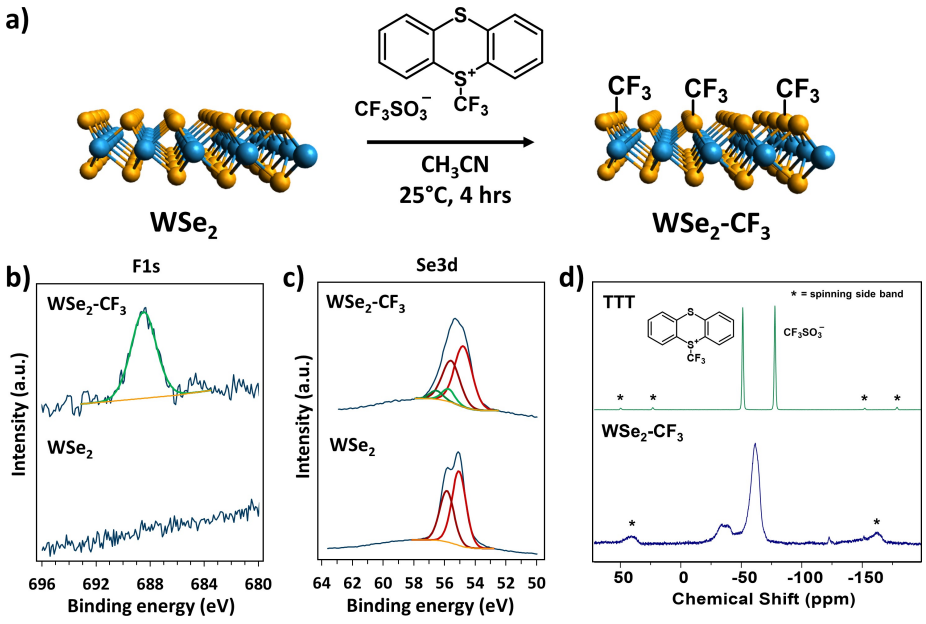

Figure 1. (a) Reaction scheme for chemical functionalization of 2D WSe_2 with trifluoromethyl thianthrenium triflate (TTT). (b) F1s and (c) Se3d XPS spectra for liquid-phase exfoliated WSe_2 before and after functionalization with TTT (25 °C, 4 hours, 10 mM in CH_3CN). (d) ^{19}F MAS NMR spectra of the starting reagent TTT and functionalized WSe_2-CF_3. Spinning side band peaks, an artifact of the measurement technique, are indicated by stars.

concentrations. The spectrum of the starting material TTT contains sharp peaks at −51 ppm and −78 ppm, corresponding to trifluoromethyl thianthrenium and the triflate counterion, respectively. These peaks are absent in the functionalized WSe_2-CF_3 spectrum, confirming that the starting material is completely removed by the post-reaction washing step. WSe_2-CF_3 shows two major peaks centered at −62 ppm and −35 ppm (Figure 1d), both of which fall within the expected region for CF_3 moieties.[34–37] The strong shifts from the starting material peak positions substantiate the formation of a new covalent bond to the CF_3 groups.

The presence of multiple peaks in the ^{19}F NMR indicates that multiple fluorine-containing species are present in-WSe_2-CF_3. We hypothesize that these structures originate from the binding of CF_3 at different sites on the surface of WSe_2. Among the possible defects in WSe_2, isolated selenium vacancies (V_{Se}) have the lowest energy of formation, but tend to react with ambient O_2 to create oxygen substitutions (O_{Se}).[38] As a result, the two most common binding sites available on the surface of WSe_2 under ambient conditions are Se atoms and O_{Se} defects. Although second-order nuclear shielding effects complicate the interpretation of chemical shifts in ^{19}F NMR,[39] empirical trends in reported small-molecule NMR spectra show that O–CF_3 groups generally appear in the −55 ppm to −60 ppm range, while Se–CF_3 groups fall in the −30 ppm to −40 ppm range.[34–36] Therefore, we assign the peaks at −35 ppm and −62 ppm to CF_3 moieties bound to Se and O_{Se} sites, respectively.

We next investigated the effects of the trifluoromethylation methodology on monolayer and few-layer single flakes by preparing and functionalizing mechanically exfoliated WSe_2 samples on 300 nm Si/SiO_2. The samples were functionalized by immersion in a 10 mM TTT solution in acetonitrile for 4 hours, then washed vigorously with acetonitrile to remove any weakly physisorbed material. The chemical composition of the deposited layer was then probed using spatially resolved ToF-SIMS, which is a highly surface-sensitive technique that detects elements and molecular fragments in the upper 1–2 nm of a surface. Figure 2a shows intensity maps for selected mass peaks on a WSe_2-CF_3 flake. The Se^- signal indicates the location of the WSe_2 flake in contrast to the SiO_2 substrate background. The flake surface shows the presence of F^-, CF_3^-, and triflate mass fragments, further supporting the reaction scheme proposed in Figure 1a. These species are notably absent on the SiO_2 substrate, indicating that the reaction is selective for WSe_2. We note that the secondary ion yields in SIMS vary widely with the sample and fragment in question, so the relative intensity of each mass signal does not necessarily correspond to its abundance in the sample.[40] Notably, triflate shows a strong signal in SIMS but is absent in the ^{19}F NMR, which implies that this species is present only in trace quantities. The presence of CF_3 groups, however, is supported by strong signals in ^{19}F NMR.

ToF-SIMS was also used to investigate the thermal stability of WSe_2-CF_3. Mechanically exfoliated flakes treated with TTT were measured after annealing in nitrogen. ToF-SIMS mapping shows no change in the F^- or CF_3^- signals up to 200 °C (Figure S2). The $SO_3CF_3^-$ signal decreases sharply at 200 °C and disappears entirely at 300 °C, indicating the removal of physisorbed triflate groups. The CF_3^- signal also decreases at 300 °C but the F^- signal remains, indicating that fluorine-containing degradation products of the trifluoromethyl groups remain on the WSe_2 surface.

Figures 2b and 2c show AFM images of mechanically exfoliated WSe_2 flakes before and after trifluoromethylation. The functionalized flakes show an increase in height

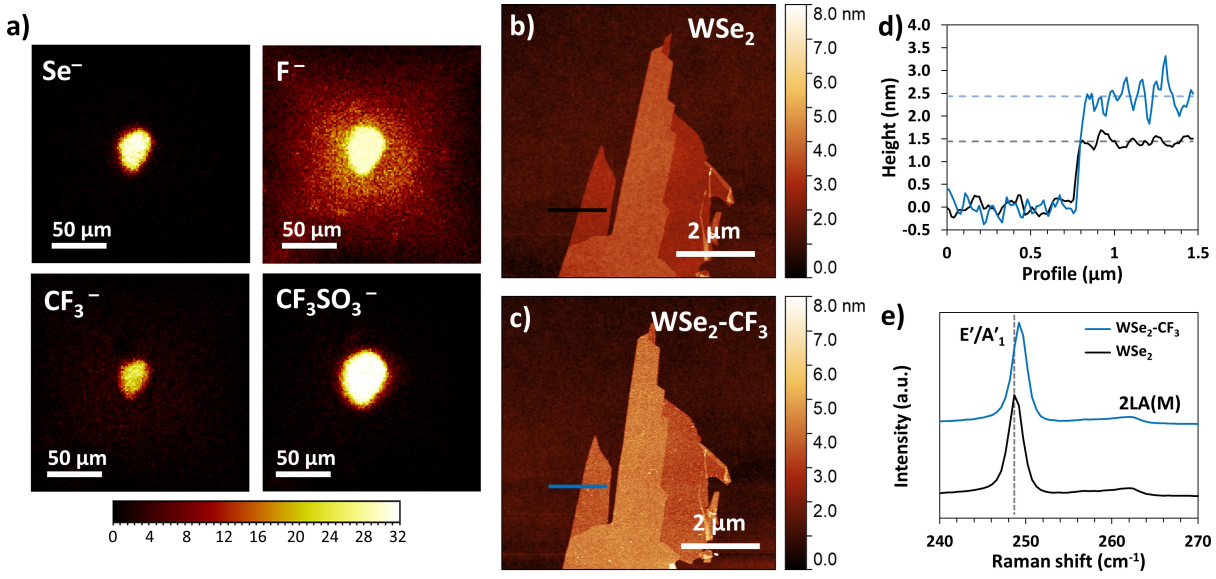

Figure 2. (a) Static ToF-SIMS maps of Se^-, F^-, CF_3^-, and $CF_3SO_3^-$ mass signals on mechanical exfoliated WSe_2 following functionalization with TTT (25 °C, 4 hours, 10 mM in CH_3CN). (b, c) AFM images of mechanically exfoliated WSe_2 (b) and WSe_2-CF_3 (c). (d) Height profiles extracted along the black and blue lines in the AFM images of pristine and functionalized WSe_2 show an increase in height due to the presence of an adlayer. (e) Raman spectra of mechanically exfoliated monolayer WSe_2-CF_3 shows a blue shift in the E'/A'_1 mode due to p-type doping.

and surface roughness, consistent with the selective surface functionalization of the 2D material. The measured height change, around 1 nm, is greater than the height of the CF_3 groups alone, which is expected to be between 2 Å and 3 Å.[41] The discrepancy in height is attributed to differences in tip-sample interactions between the pristine WSe_2, the CF_3 adlayer, and the surrounding SiO_2, which introduce error into AFM step height measurements.[42]

The integrity of the underlying monolayer WSe_2 was next probed with Raman spectroscopy. As shown in Figure 2e, monolayer WSe_2 exhibits overlapping Raman modes at 249 cm^{-1} (A_1') and 251 cm^{-1} (E′), while a broad peak near 263 cm^{-1} corresponds to the disorder-activated 2LA(M) mode.[43] Following functionalization, the 2LA(M) peak does not noticeably change in intensity, indicating that the surface treatment does not induce significant disorder in the WSe_2 lattice (Figure 2e). The E′-A_1' peak shows a slight blue shift of about 0.7 cm^{-1}, which is consistent with p-type doping.[44,45]

The doping trend agrees with the proposed reaction scheme given in Figure 3a, in which Se donates a pair of electrons to the electrophilic CF_3 group with loss of neutral thianthrene. This results in a positive charge on the Se atom, which creates a strong hole-doping effect in the surrounding WSe_2 lattice. In addition, the strongly dipolar CF_3 groups plausibly generate a local electric field at the WSe_2 surface. This dipole interaction produces a local gating effect, shifting the conduction band of WSe_2 toward the Fermi level.[3] An analogous scheme and doping effect is expected to involve the O_{Se} sites, where substitutional oxygen takes the place of Se.

To assess the validity of the proposed configurations of CF_3 on WSe_2, three plausible binding sites were investigated using high-level DFT. Figures 3b–d show the calculated binding energy, band structure, and projected density of states (PDOS) for WSe_2 with CF_3 bound at Se, O_{Se}, and V_{Se} sites. The reaction is predicted to be exergonic for all three structures, with Se sites showing the highest binding energy of 1.16 eV. In the case of both Se and O_{Se}, the binding of the CF_3 group introduces a localized state near the conduction band. The band gap for the Se sites shows a direct-to-indirect transition upon functionalization, while O_{Se} remains direct. In the case of V_{Se}, localized states already exist at the vacancy site and show little change upon functionalization.

To test the effect of trifluoromethylation on the charge transport properties of WSe_2, we fabricated back-gated FETs using mechanically exfoliated WSe_2 on Si/SiO_2 (Figure 4a). The pristine devices are ambipolar with substantial electron transport ($\mu_e = 22.7$ cm^2/Vs) and poor hole transport ($\mu_h = 0.0015$ cm^2/Vs). Upon exposure to TTT, hole transport is enhanced while electron transport decreases, indicating p-type doping of WSe_2. After 24 hours of reaction time, hole transport reaches as high as 0.75 cm^2/Vs while electron transport falls to 7.6 cm^2/Vs. The observation of tunable p-type doping supports the electrophilic reaction mechanism proposed in Figure 3a and provides proof of concept for the use of TTT as an effective surface dopant.

We further probed the thermal stability of the CF_3 adsorbates by annealing the FETs under inert conditions. The functionalization-induced increase in hole transport is partially reversed upon annealing, which is attributed to the removal of physisorbed surface species such as residual

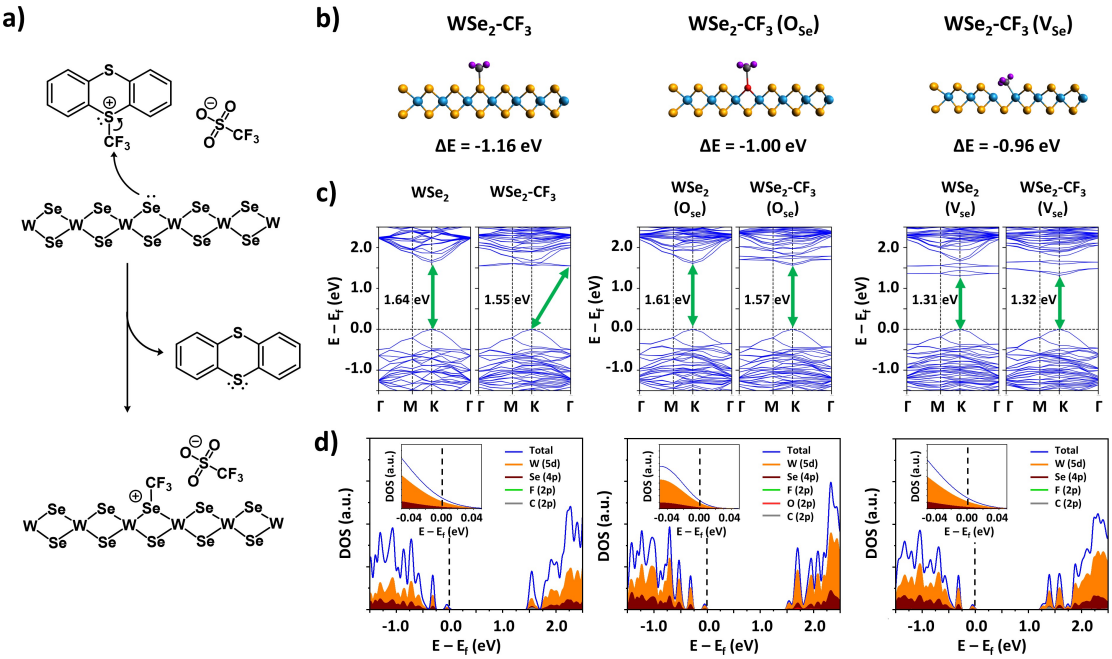

Figure 3. (a) Proposed mechanism for the reaction of TTT with WSe_2. (b) Proposed structures for CF_3 bound to Se, O_{Se}, and V_{Se} on the surface of WSe_2. The calculated binding energy at each site (ΔE for the reaction) is given below each structure. (c) Band structures for each indicated structure before and after the reaction. (d) Projected density of states for each of the three functionalized structures. Inset shows the valence band edge.

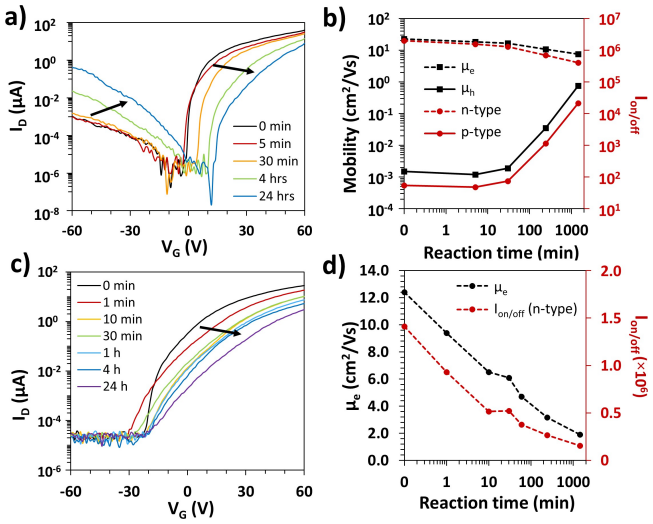

Figure 4. (a) Transfer curves and (b) transistor metrics of a few-layer WSe_2 FET at increasing reaction times with TTT ($V_D = 5$ V). (c) Transfer curves and (d) transistor metrics of a multilayer MoS_2 FET at increasing reaction times with TTT ($V_D = 1$ V) Hole mobility (μ_h) and p-type on-off ratios ($I_{on/off}$) are calculated from the low-V_G region of each curve, while electron mobility (μ_e) and n-type $I_{on/off}$ are calculated from the high-V_G regions.

solvent molecules. However, hole transport remains higher than the pristine WSe_2 device even under annealing up to 300 °C, reflecting the strong covalent bonding and stable hole doping by the CF_3 groups (Figure S3). At 300 °C, ToF-SIMS data indicates that the CF_3 groups begin to break down. In the FET measurements, a slight increase in hole transport occurs at the same temperature, indicating that the degradation products of CF_3 also act as hole dopants.

Low-temperature PL measurements were carried out to assess the effect of trifluoromethylation on the optical properties of WSe_2. Monolayer WSe_2 flakes were prepared by mechanical exfoliation and measured before and after functionalization with 532 nm excitation at 4 K. Figure S4 shows a representative point spectrum. The pristine material shows a number of emission features corresponding to the neutral exciton (X_0) and negatively charged trions (X_1^-, X_2^-).[46–48] Following functionalization, these features are strongly suppressed, while a new peak appears at 730 nm. This peak is identified as the positive trion (X^+), which is typically observed as a result of hole doping.[46–48] These results corroborate the trends shown in the transport measurements and indicate the value of trifluoromethylation as a strategy to modulate the optical emission of TMDCs.

The emission measurements point to potential applications of trifluoromethylation. We note that TTT shows relatively weak doping efficiency in comparison to other surface dopants (Table S1).[3] While not ideal for CMOS technology, mild doping can be used to effectively modify the relative abundance of emissive excitonic species in WSe_2. This control over the emission spectrum is highly desirable for quantum communication and other optoelectronics applications.[9,10,45] For these areas of study, it is also vital to identify specific structural features that produce a particular emission profile. In this respect, trifluoromethylation stands out among other organic surface dopants for its well-characterized reactivity. The simple structure of the CF_3 group and the presence of fluorine heteroatoms have enabled us to identify how CF_3 groups bond to the surface and suggest mechanisms for doping. We suggest that TTT can enable rigorous mechanistic understanding of the effect of organic functionalization on the emission properties of TMDCs in future studies.

To illustrate the versatility of this trifluoromethylation protocol, it was next replicated for 2D MoS_2. Figure 4c shows representative transfer curves for a bilayer MoS_2 FET functionalized with TTT. The FETs show only n-type transport ($\mu_e = 12.4$ cm^2/Vs), which is suppressed with increasing reaction time to $\mu_e = 1.9$ cm^2/Vs after 24 hours (Figure 4). The diminished n-type character reflects the depletion of electron density in MoS_2 due to electron transfer in the electrophilic reaction mechanism (Figure 3a) as well as local gating by the CF_3 groups.

Chemical characterization for MoS_2-CF_3 largely mirrors that of WSe_2-CF_3. ToF-SIMS, AFM, and XPS data show the preferential deposition of a thin layer of fluorine-containing material on the surface of MoS_2 flakes (Figure S5–S7). The appearance of a new doublet in the S2p XPS spectrum indicates covalent binding between the MoS_2 and CF_3. Quantification of the S2p and F1s peaks on a large-area monolayer sample indicates a density of around 1 CF_3 group per 12 MoS_2 unit cells, similar to that for WSe_2 (Figure S8).

The MoS_2-CF_3 solid-state ^{19}F MAS NMR spectrum shows the disappearance of peaks corresponding to TTT and the appearance of a peak at −62 ppm, indicating covalent binding of CF_3 groups (Figure S9). Upon increasing the reaction temperature to 75 °C, a second peak appears at −33 ppm. Similar to WSe_2, the most common defect sites in MoS_2 are reported to be oxygen substitutions (O_S).[49] The peaks at −33 ppm and −62 ppm are assigned to CF_3 groups bound to S and O_S sites, respectively, in line with the chemical shift ranges for S–CF_3 and O–CF_3 groups reported in literature.[34–37] The fact that the S-CF_3 peak is only observed following the high-temperature reaction indicates that S sites on the surface of MoS_2 are less reactive toward electrophilic trifluoromethylation compared to Se sites in WSe_2, although O_S sites react readily. Computational results corroborate this hypothesis, since O_S sites show a higher binding affinity for CF_3 groups compared to the pristine MoS_2 surface (Figure S10). These results indicate that TTT can act as a versatile functionalization reagent for MoS_2 as well as WSe_2, and the present fundamental characterization provides key insight into the binding of electrophilic groups on the surface of the TMDCs.

Conclusions

Here we have demonstrated the covalent functionalization of 2D TMDCs, WSe_2 and MoS_2, with trifluoromethyl groups. TTT acts as a mild and efficient electrophilic trifluoromethylation reagent which can be prepared and used by straightforward procedures. Detailed chemical character-

ization and DFT computation data support the formation of covalent bonds between CF_3 groups and surface chalcogens or oxygen substitutions. Proof-of-concept charge transport measurements demonstrate that trifluoromethylation induces p-type doping that can be tuned with reaction time. This doping can also be used to modulate the optical emission of WSe_2 by promoting the formation of positive trions. Overall, this work illustrates that electrophilic trifluoromethylation provides a promising straightforward solution-based method for controlling the electronic and optical properties of 2D WSe_2 and MoS_2.

Supporting Information

The Supporting Information contains additional details on experimental and computational methods as well as computational and experimental analysis data for WSe_2-CF_3 and MoS_2-CF_3.

Acknowledgements

This work was primarily supported by the Materials Research Science and Engineering Center of Northwestern University (NSF DMR-2308691). Additional support was provided by the U.S. Department of Commerce, National Institute of Standards and Technology (Award 70NANB19H005) as part of the Center for Hierarchical Materials Design (CHiMaD) (B.K.). Theory and experimental work (T.S., L.O.J., G.C.S., R.L.A.) was supported by the Center for Molecular Quantum Transduction, an Energy Frontier Research Center funded by the U.S. Department of Energy (DOE), Office of Science, Basic Energy Sciences (BES), under Award # (DE-SC0021314). A.D. acknowledges the National Science Foundation (NSF) for a Graduate Research Fellowship. A.F. acknowledges NSF grant DMR-2223922 for support. This work made use of the IMSERC NMR and MS facilities at Northwestern University, which have received support from the Soft and Hybrid Nanotechnology Experimental (SHyNE) Resource (NSF ECCS-2025633), International Institute of Nanotechnology (IIN), and Northwestern University. This work also made use of the Keck-II and NUFAB facilities of Northwestern University's NUANCE Center, which has received support from the SHyNE Resource (NSF ECCS-2025633), the IIN, and Northwestern's MRSEC program (NSF DMR-2308691).

Conflict of Interest

The authors declare no conflict of interest.

Data Availability Statement

The data that support the findings of this study are available in the supplementary material of this article.

Keywords: WSe_2 · MoS_2 · trifluoromethylation · functionalization

[1] V. K. Sangwan, M. C. Hersam, *Annu. Rev. Phys. Chem.* **2018**, *69*, 299–325.
[2] M. C. Lemme, D. Akinwande, C. Huyghebaert, C. Stampfer, *Nat. Commun.* **2022**, *13*, 1392.
[3] Y. Zhao, M. Gobbi, L. E. Hueso, P. Samorì, *Chem. Rev.* **2022**, *122*, 50–131.
[4] D. Jariwala, T. J. Marks, M. C. Hersam, *Nat. Mater.* **2017**, *16*, 170–181.
[5] P.-C. Shen, C. Su, Y. Lin, A.-S. Chou, C.-C. Cheng, J.-H. Park, M.-H. Chiu, A.-Y. Lu, H.-L. Tang, M. M. Tavakoli, G. Pitner, X. Ji, Z. Cai, N. Mao, J. Wang, V. Tung, J. Li, J. Bokor, A. Zettl, C.-I. Wu, T. Palacios, L.-J. Li, J. Kong, *Nature* **2021**, *593*, 211–217.
[6] Y. Wang, J. C. Kim, Y. Li, K. Y. Ma, S. Hong, M. Kim, H. S. Shin, H. Y. Jeong, M. Chhowalla, *Nature* **2022**, *610*, 61–66.
[7] L. Kong, X. Zhang, Q. Tao, M. Zhang, W. Dang, Z. Li, L. Feng, L. Liao, X. Duan, Y. Liu, *Nat. Commun.* **2020**, *11*, 1866.
[8] Y. Wang, J. C. Kim, R. J. Wu, J. Martinez, X. Song, J. Yang, F. Zhao, A. Mkhoyan, H. Y. Jeong, M. Chhowalla, *Nature* **2019**, *568*, 70–74.
[9] X. Liu, M. C. Hersam, 2D materials for quantum information science. *Nat. Rev. Mater.* **2019**, *4(10)*, 669–684.
[10] M. I. B. Utama, H. Zeng, T. Sadhukhan, A. Dasgupta, S. C. Gavin, R. Ananth, D. Lebedev, W. Wang, J.-S. Chen, K. Watanabe, T. Taniguchi, T. J. Marks, X. Ma, E. A. Weiss, G. C. Schatz, N. P. Stern, M. C. Hersam, *Nat. Commun.* **2023**, *14*, 2193.
[11] S. H. Amsterdam, T. J. Marks, M. C. Hersam, *J. Phys. Chem. Lett.* **2021**, *12*, 4543–4557.
[12] L. O. Jones, M. A. Mosquera, M. A. Ratner, G. C. Schatz, *ACS Appl. Mater. Interfaces* **2020**, *12*, 4607–4615.
[13] Y. Zhao, K. Xu, F. Pan, C. Zhou, F. Zhou, Y. Chai, *Adv. Funct. Mater.* **2017**, *27*, 1603484.
[14] C. R. Ryder, J. D. Wood, S. A. Wells, Y. Yang, D. Jariwala, T. J. Marks, G. C. Schatz, M. C. Hersam, *Nat. Chem.* **2016**, *8*, 597–602.
[15] S. H. Amsterdam, T. K. Stanev, Q. Zhou, A. J. T. Lou, H. Bergeron, P. Darancet, M. C. Hersam, N. P. Stern, T. J. Marks, *ACS Nano* **2019**, *13*, 4183–4190.
[16] S. Padgaonkar, S. H. Amsterdam, H. Bergeron, K. Su, T. J. Marks, M. C. Hersam, E. A. Weiss, *J. Phys. Chem. C* **2019**, *123*, 13337–13343.
[17] S. H. Amsterdam, T. K. Stanev, L. Wang, Q. Zhou, S. Irgen-Gioro, S. Padgaonkar, A. A. Murthy, V. K. Sangwan, V. P. Dravid, E. A. Weiss, P. Darancet, M. K. Y. Chan, M. C. Hersam, N. P. Stern, T. J. Marks, *J. Am. Chem. Soc.* **2021**, *143*, 17153–17161.
[18] H. Fang, M. Tosun, G. Seol, T. C. Chang, K. Takei, J. Guo, A. Javey, *Nano Lett.* **2013**, *13*, 1991–1995.
[19] H. Fang, S. Chuang, T. C. Chang, K. Takei, T. Takahashi, A. Javey, *Nano Lett.* **2012**, *12*, 3788–3792.
[20] W. Liu, J. Kang, D. Sarkar, Y. Khatami, D. Jena, K. Banerjee, *Nano Lett.* **2013**, *13*, 1983–1990.
[21] L. Yu, A. Zubair, E. J. G. Santos, X. Zhang, Y. Lin, Y. Zhang, T. Palacios, *Nano Lett.* **2015**, *15*, 4928–4934.
[22] D. Voiry, A. Goswami, R. Kappera, C. d. C. C. e. Silva, D. Kaplan, T. Fujita, M. Chen, T. Asefa, M. Chhowalla, *Nat. Chem.* **2015**, *7*, 45–49.
[23] S. Manjunatha, S. Rajesh, P. Vishnoi, C. N. R. Rao, *J. Mater. Res.* **2017**, *32*, 2984–2992.
[24] E. X. Yan, M. Cabán-Acevedo, K. M. Papadantonakis, B. S. Brunschwig, N. S. Lewis, *ACS Materials Lett.* **2020**, *2*, 133–139.

[25] K. C. Knirsch, N. C. Berner, H. C. Nerl, C. S. Cucinotta, Z. Gholamvand, N. McEvoy, Z. Wang, I. Abramovic, P. Vecera, M. Halik, S. Sanvito, G. S. Duesberg, V. Nicolosi, F. Hauke, A. Hirsch, J. N. Coleman, C. Backes, *ACS Nano* **2015**, *9*, 6018–6030.
[26] X. S. Chu, A. Yousaf, D. O. Li, A. A. Tang, A. Debnath, D. Ma, A. A. Green, E. J. G. Santos, Q. H. Wang, *Chem. Mater.* **2018**, *30*, 2112–2128.
[27] H. G. Ji, P. Solís-Fernández, D. Yoshimura, M. Maruyama, T. Endo, Y. Miyata, S. Okada, H. Ago, *Adv. Mater.* **2019**, *31*, 1903613.
[28] M. Vera-Hidalgo, E. Giovanelli, C. Navío, E. M. Pérez, *J. Am. Chem. Soc.* **2019**, *141*, 3767–3771.
[29] R. Quirós-Ovies, M. Vázquez Sulleiro, M. Vera-Hidalgo, J. Prieto, I. J. Gómez, V. Sebastián, J. Santamaría, E. M. Pérez, *Chem. Eur. J.* **2020**, *26*, 6629–6634.
[30] J. Miao, L. Wu, Z. Bian, Q. Zhu, T. Zhang, X. Pan, J. Hu, W. Xu, Y. Wang, Y. Xu, B. Yu, W. Ji, X. Zhang, J. Qiao, P. Samorì, Y. Zhao, *ACS Nano* **2022**, *16*, 20647–20655.
[31] H. Jia, A. P. Häring, F. Berger, L. Zhang, T. Ritter, *J. Am. Chem. Soc.* **2021**, *143*, 7623–7628.
[32] J. Kang, S. A. Wells, V. K. Sangwan, D. Lam, X. Liu, J. Luxa, Z. Sofer, M. C. Hersam, *Adv. Mater.* **2018**, *30*, 1802990.
[33] National Institute of Standards and Technology, "NIST X-Ray Photoelectron Spectroscopy Database", can be found under can be found under https://srdata.nist.gov/xps, **2012** (accessed: June 19, 2023).
[34] ACS Division of Organic Chemistry, "Hans Reich's Collection. NMR Spectroscopy", can be found at https://organicchemistry-data.org/ hansreich/resources/nmr **2023** (accessed June 24, 2023).
[35] S. R. Mudshinge, Y. Yang, B. Xu, G. B. Hammond, Z. Lu, *Angew. Chem. Int. Ed.* **2022**, *61*, e202115687.
[36] J. Grobe, R. Haubold, *Z. Anorg. Allg. Chem.* **1985**, *522*, 159–170.
[37] M.-L. Abasq, F. Y. Pétillon, J. Talarmin, *J. Chem. Soc. Chem. Commun.* **1994**, 2191–2192.
[38] Y. J. Zheng, Y. Chen, Y. L. Huang, P. K. Gogoi, M.-Y. Li, L.-J. Li, P. E. Trevisanutto, Q. Wang, S. J. Pennycook, A. T. S. Wee, S. Y. Quek, *ACS Nano* **2019**, *13*, 6050–6059.
[39] J. N. Dahanayake, C. Kasireddy, J. P. Karnes, R. Verma, R. M. Steinert, D. Hildebrandt, O. A. Hull, J. M. Ellis, K. R. Mitchell-Koch, in *Annual Reports on NMR Spectroscopy, Vol. 93* (Ed.: G. A. Webb), Academic Press, **2018**, pp. 281–365.
[40] P. van der Heide, *Secondary Ion Mass Spectrometry: An Introduction to Principles and Practices*, John Wiley and Sons, Inc., Hoboken, NJ, **2014**.
[41] National Institute of Standards and Technology, "NIST Computational Chemistry Comparison and Benchmark Database", can be found under https://cccbdb.nist.gov, **2022** (accessed October 27, 2023).
[42] K. Godin, C. Cupo, E.-H. Yang, *Sci. Rep.* **2017**, *7*, 17798.
[43] E. del Corro, H. Terrones, A. Elias, C. Fantini, S. Feng, M. A. Nguyen, T. E. Mallouk, M. Terrones, M. A. Pimenta, *ACS Nano* **2014**, *8*, 9629–9635.
[44] B. Chakraborty, A. Bera, D. V. S. Muthu, S. Bhowmick, U. V. Waghmare, A. K. Sood, *Phys. Rev. B* **2012**, *85*, 161403.
[45] D.-H. Kang, J. Shim, S. K. Jang, J. Jeon, M. H. Jeon, G. Y. Yeom, W.-S. Jung, Y. H. Jang, S. Lee, J.-H. Park, *ACS Nano* **2015**, *9*, 1099–1107.
[46] Z. Li, T. Wang, Z. Lu, C. Jin, Y. Chen, Y. Meng, Z. Lian, T. Taniguchi, K. Watanabe, S. Zhang, D. Smirnov, S.-F. Shi, Revealing the biexciton and trion-exciton complexes in BN encapsulated WSe2. *Nat. Commun.* **2018**, *9(1)*, 3719.
[47] Z. Li, T. Wang, C. Jin, Z. Lu, Z. Lian, Y. Meng, M. Blei, S. Gao, T. Taniguchi, K. Watanabe, T. Ren, S. Tongay, L. Yang, D. Smirnov, T. Cao, S.-F. Shi, Emerging photoluminescence from the dark-exciton phonon replica in monolayer WSe2. *Nat. Commun.* **2019**, *10(1)*, 2469.
[48] M. He, P. Rivera, D. Van Tuan, N. P. Wilson, M. Yang, T. Taniguchi, K. Watanabe, J. Yan, D. G. Mandrus, H. Yu, H. Dery, W. Yao, X. Xu, Valley phonons and exciton complexes in a monolayer semiconductor. *Nat. Commun.* **2020**, *11(1)*, 618.
[49] S. Barja, S. Refaely-Abramson, B. Schuler, D. Y. Qiu, A. Pulkin, S. Wickenburg, H. Ryu, M. M. Ugeda, C. Kastl, C. Chen, C. Hwang, A. Schwartzberg, S. Aloni, S.-K. Mo, D. Frank Ogletree, M. F. Crommie, O. V. Yazyev, S. G. Louie, J. B. Neaton, A. Weber-Bargioni, *Nat. Commun.* **2019**, *10*, 3382.

Manuscript received: February 19, 2024
Accepted manuscript online: March 29, 2024
Version of record online: April 23, 2024